

# Capturing Shock Waves Using an Open-Source, Direct Simulation Monte Carlo (DSMC) Code

*A.O. Ahmad, T.J. Scanlon and J.M. Reese  
Department of Mechanical Engineering, University of Strathclyde  
James Weir Building, 75 Montrose Street, Glasgow G1 1XJ, U.K.*

4<sup>th</sup> - 8<sup>th</sup> July 2011

## **Abstract**

This paper presents a comparison between experimental and numerical investigations of hypersonic flows over complex geometries. Two hypersonic cases have been considered: Ma 15.6 flow over a 25°/ 55° bi-conic cylindrical object and Ma 20.2 flow over a planetary probe geometry. Experimental results are from the literature. Numerical results are from a new open-source DSMC code called *dsmcFoam*. The two cases simulated by *dsmcFoam* show good qualitative and quantitative agreement with the experimental data. This paper also presents very good agreement, between *dsmcFoam* and another DSMC code, of aerodynamic forces incurred by the Apollo Command Module.

**Nomenclature**

$C_A$	Apollo capsule: axial force coefficient, axial force/ $(0.5\rho_\infty A_{ref} V_\infty^2)$
$C_D$	Apollo capsule: drag force coefficient, drag force/ $(0.5\rho_\infty A_{ref} V_\infty^2)$
$C_L$	Apollo capsule: lift force coefficient, lift force/ $(0.5\rho_\infty A_{ref} V_\infty^2)$
$C_m$	Apollo capsule: pitching-moment coefficient, moment about $z/(0.5\rho_\infty A_{ref} V_\infty^2 D_b)$
$C_N$	Apollo capsule: normal force coefficient, normal force/ $(0.5\rho_\infty A_{ref} V_\infty^2)$
$d$	Molecular diameter
$D_b$	Apollo capsule: maximum body diameter $D_b = 2R_b$
$k$	Boltzmann constant
$L$	Length scale
$L/D$	Lift to drag ratio
$m$	Atomic mass
$Ma$	Mach number
$n$	Number density
$N_2$	Nitrogen gas
$O$	Atomic Oxygen
$O_2$	Oxygen gas
$p$	Pressure
$q$	Heating rate
$R$	Gas constant
$R_a$	Apollo capsule: afterbody spherical nose radius
$R_n$	Apollo capsule: blunt forebody spherical nose radius
$R_s$	Apollo capsule: shoulder radius
$S$	Planetary probe: distance along surface from nose radius tip
$T$	Temperature
$X$	Mole fraction
$z$	Bi-conic cylindrical object: distance from cone tip
$\alpha$	Angle of incidence
$\lambda$	Mean free path
$\mu$	Gas dynamic viscosity
$\rho$	Gas density
$\phi$	Diameter of circle
$\omega$	Temperature coefficient of viscosity

*Subscripts*

$w$	Wall quantity
$\infty$	Free-stream conditions
$0$	Stagnation conditions
$p$	Arbitrary species
$q$	Arbitrary species
$ref$	Reference value

**1. Introduction**

This paper describes the application of a new direct simulation Monte Carlo (DSMC) code, called *dsmcFoam*, to the capture of shock waves. The code has been written within the framework of the open-source computational fluid dynamics (CFD) toolbox OpenFOAM [1] that can be downloaded freely from [www.openfoam.com](http://www.openfoam.com). The main features of *dsmcFoam* are its C++ modularity, its unlimited parallel processing capability and its ability to easily handle arbitrary, complex 3D geometries. Results of initial benchmark trials [2] have shown excellent agreement with both analytical solutions and other conventional DSMC codes.

In order to extend the range of applications of *dsmcFoam*, three hypersonic test cases are considered in the present paper:

1. Ma 15.6 flow over a  $25^\circ/55^\circ$  bi-conic cylindrical object,

2. Ma 20.2 flow over a planetary probe geometry,
3. 7.7 to 15 km/s air flow over the Apollo Command Module.

These cases represent a significant challenge to numerical codes as they must capture flow physics including weak and diffuse shocks, boundary layer separation, flow recirculation, rapid expansion and re-compression, and shear layers with steep gradients of velocity, temperature and density. Furthermore, numerical codes for high speed, rarefied gas flows should also have the ability to capture shock-boundary layer and shock-shock interactions.

## 2. *dsmcFoam* characteristics

High speed vehicles which function in rarefied gas surroundings may come across non-equilibrium and non-continuum flow conditions that can have a significant influence on aerodynamic performance and vehicle surface heat flux. Numerical techniques which do not successfully capture such behaviour miss an essential part of the flow physics surrounding the vehicle. Under such conditions, a particulate method best captures the dilute flow environment.

The DSMC technique, originated by Bird [3] in the 1970s, allows particles to move and collide using kinetic-theory considerations that treat the non-equilibrium gas behaviour accurately. DSMC considers molecular collisions using stochastic rather than deterministic procedures and each DSMC particle represents a large number of real gas molecules. The decoupling of particle ballistic motion and particle collisions improves the computational efficiency of DSMC greatly in comparison with other particulate methods such as molecular dynamics (MD). As a result, the DSMC technique is the dominant numerical method for applications involving rarefied gas flow.

The DSMC code *dsmcFoam* is available in the latest version of OpenFOAM, which is freely obtainable and open source under the GNU general public licence. *dsmcFoam* originated from the core characteristics of a MD code implemented by some of the present authors in the OpenFOAM toolbox. The core characteristics of *dsmcFoam* include particle initialisation in arbitrary geometries and particle tracking in unstructured, arbitrary, polyhedral meshes.

Molecular collisions in *dsmcFoam* are simulated using the variable hard sphere (VHS) model [4], with the Larsen-Borgnakke phenomenological model [3] governing the energy exchange between kinetic and internal modes; for the present paper, energy is exchanged between translational and rotational modes only, and non-reacting gas models are used. The mean free path  $\lambda$ , for a single-species (SS)  $\lambda_{SS}$ , and multi-species (MS)  $\lambda_{MS}$  are determined through:

$$\lambda_{SS} = (2\mu/15\rho)(5 - 2\omega)(7 - 2\omega)(2\pi RT)^{-1/2}, \quad (1)$$

$$\lambda_{MS} = \sum_{p=1}^s \frac{n_p}{n} \left[ \sum_{q=1}^s \left\{ \pi(d_{ref})_{pq}^2 n_q \left( \frac{(T_{ref})_{pq}}{T} \right)^{\omega_{pq}^{-0.5}} \left( 1 + \frac{m_p}{m_q} \right)^{0.5} \right\} \right]^{-1}. \quad (2)$$

## 3. Simulation methodology

Experimental investigations, to obtain surface heating rates and pressure measurements, were performed by Holden *et al.* [5][6] for Ma 15.6 flow of N<sub>2</sub> over a 25°/ 55° bi-conic cylindrical object. The bi-conic configuration is illustrated in figure 1 and the free-stream experimental conditions are shown in table 1. Numerical input parameters are given in tables 2 and 3.

The planetary probe, considered as a test case model by AGARD<sup>1</sup>, is a 70° spherically-blunted cone mounted on a cylindrical sting as illustrated in figure 2. The forebody configuration is identical to that of the Mars Pathfinder probe. Allègre *et al.* [7, 8, 9] conducted experiments to obtain density flowfields, drag coefficients and surface heat transfer in the SR3 low-density wind tunnel of the Centre National de la Recherche Scientifique, for Ma 20.2 flow of N<sub>2</sub> over the planetary probe. The flow conditions, along with numerical parameters used in the *dsmcFoam* simulation, are shown in tables 1, 2 and 3. Three numerical simulations were run for the planetary probe at zero-degree angle of attack, as a different surface temperature was required for each investigation, as listed in table 3. *dsmcFoam* simulations were also carried out over the positive and negative 10-degree angle of attack planetary probe, using the same free-stream conditions in tables 1 and 3. The length scales presented in table 1 are the radius of the 25° section of the bi-conic cylindrical object, and the radius of the forebody configuration of the planetary probe.

<sup>1</sup>Advisory Group for Aerospace Research and Development (AGARD) Fluid Dynamics Panel and its Working Group 18.

Simulations to study the effects of free-stream velocity on the aerodynamic forces were carried out for the Apollo Command Module at an altitude of 105 km and -25 degrees incidence. Five free-stream velocities, ranging from 7.7 to 15 km/s (table 4), were used in this investigation and the highest velocity corresponds to the upper bounds for a Mars return mission. The Apollo capsule consists of a truncated spherical section, followed by a toroidal section, and then a conical section as shown in figure 3, while figure 4 shows the aerodynamic forces in the pitch plane. The flow conditions at an altitude of 105 km, along with numerical parameters used in the investigation are shown in tables 2, 4 and 5. The free-stream hard sphere Knudsen number is 0.081, where the length scale is based on the maximum body diameter  $D_b$ .

Both, bi-conic cylindrical object and planetary probe, cases were modelled as three-dimensional quarter-section models whereas the Apollo capsule case was modelled as a three-dimensional half-section model. All cases were run with symmetry boundary conditions, as *dsmcFoam* does not currently have an axisymmetric capability. With the use of the meshing utilities *blockMesh* and *snappyHexMesh*, available within the OpenFOAM toolbox [1], the three cases with complex geometries were meshed with ease. For good DSMC practice the mesh size is smaller than  $\lambda$ , and the numerical time-step is smaller than the mean-free-time. When the simulation has reached steady state, time-averaging is started for a period roughly equal to 5 times the duration to steady state. The bi-conic case takes longer to resolve due to the complex nature of the flow physics, involving a shock-shock interaction, in this instance compared with the planetary probe. Numerical calculations were performed on Strathclyde University's Engineering Faculty High Performance Computer (1088 cores, 100TB disk storage, 13 TeraFlops peak performance).

## 4. Results and discussion

This section describes the comparisons between *dsmcFoam* and results from literature described in the previous section, of the three hypersonic test cases.

### 4.1 Bi-conic test case

Experimental [5][6] measurements of surface heating rates and pressure on the bi-conic cylindrical object are compared with the data obtained from *dsmcFoam* in figures 5 and 6. The *dsmcFoam* pressure data shows a reasonable concurrence with the experimental data. The agreement is less evident for the heat flux in the 25° section of the bi-conic cylindrical object but improves in the 55° section.

Within the shock-shock interaction, which occurs at  $z \approx 0.1$  m, a higher surface heating rate has been observed from *dsmcFoam* in comparison to the experiment. To adequately resolve the surface heating rate in the shock-shock interaction a refined mesh is required in this region. Further DSMC studies will reduce the noise in the surface heating rate and pressure values by using more simulated particles.

### 4.2 Planetary probe test case

Dimensionless density flowfields from the experimental observations of Allègre *et al.* [7], and *dsmcFoam* results are presented in figures 7, 8 and 9 for zero angle of attack, positive and negative 10 degree angle of attack respectively. The contour plots show a very good agreement between experiment and *dsmcFoam*. The maximum density occurs in the stagnation region directly in front of the object, with a maximum relative density of approximately 16 for the zero angle of attack planetary probe. The bow shock structure upstream of the forebody has been particularly well captured. The largest area of discrepancy appears in the wake region immediately downstream of the forebody, adjacent to the sting. This zone has highly rarefied flow so, in order to adequately resolve the flow-field in this area, a coarser mesh is required. Further DSMC studies will assess the mesh sensitivity in this area.

Comparisons of surface heat transfer between experiment [9] and *dsmcFoam* are shown in figure 10. Very good agreement is observed at the different thermocouple locations, illustrated in figure 10. Some discrepancies appear in the highly-rarefied region (at thermocouple locations 5 and 6). However, Allègre *et al.* [9] state that there is a degree of experimental uncertainty in this region due to the difficulty in accurately measuring such low heat fluxes. This makes it difficult to ascertain the level of numerical-experimental agreement in this area.

The experimental [8] drag coefficient, for zero degree angle of attack, is 1.657. In comparison, *dsmcFoam* has predicted 1.89. Although this is a reasonable agreement, further grid, time-step and particle number sensitivity analyses are required to optimise the DSMC results. Furthermore, the results presented in this paper are based on particle collisions involving energy exchange between the translational and rotational modes only. However, the maximum

overall temperatures encountered in the planetary probe and bi-conic cases were 1011 K and 2389 K, respectively. Under such conditions the excitation of the vibrational energy mode requires to be included in order to capture the correct flow physics. This is currently being incorporated into *dsmcFoam*.

### 4.3 Apollo Command Module

*dsmcFoam* results presented in figures 11 and 12, of the 5 free-stream velocities, show that the aerodynamic coefficients change with increasing velocity. They change in a similar fashion to those being subject to increasing rarefaction, presented by Moss *et al.* [10]. In other words, the coefficients of lift force and lift-to-drag (L/D) ratio decrease with increasing free-stream velocity and the coefficients of drag, normal and axial force increase with increasing velocity. Also, presented in figures 11 and 12 are the Apollo capsule aerodynamic coefficients of Moss *et al.*, for several free-stream velocities, using the DS3V program of Bird [11]. Between the *dsmcFoam* and Moss *et al.* results, the lift-to-drag ratio and coefficients of lift and normal force are in very good agreement. The drag and axial force coefficients are also in good agreement, with a maximum difference of ~4% between the results.

## 5. Mesh decomposition investigation

Effective computational domain decomposers, for parallel processing, play a vital tool for the efficiency of any solver in particular for computationally demanding techniques such as DSMC. Previous decomposition methods used for *dsmcFoam* were either the *Simple* or *Scotch* techniques, available in OpenFOAM [1]. They are based on splitting the computational domain into sections by direction or by automatic decomposition respectively. The *Scotch* technique splits the domain so that each processor has the same number of cells to work with whilst minimising processor boundaries and requires no geometric input.

In order to increase the computational efficiency of *dsmcFoam*, we have developed and tested an extension to the *Scotch* decomposer. This new decomposer splits the domain so that each processor has the same number of particles to work with, meaning that processors are concentrated in regions of high number of particles, for example, in shock waves.

To assess the new *Scotch* technique, which is open-source and available from the OpenFOAM website (version 1.7.x), all three decomposers were tested on the zero angle of attack planetary probe case mentioned in section 4. The efficiency of all three decomposers, shown on figure 13, shows that the new *Scotch* technique has greatly increased the computational saving. Using the new *Scotch* method with 64 processors the computational time is reduced by 28% and 35% in comparison with the standard *Scotch* and *Simple* techniques, respectively.

## 6. Conclusions

We have presented benchmark trials of a new, open-source DSMC code called *dsmcFoam*. The code has been written within the framework of the open-source numerical analysis toolbox OpenFOAM. The principal features of *dsmcFoam* are its C++ modularity, its unlimited parallel processing capability and its ability to easily handle arbitrary, complex 3D geometries.

Results for initial benchmark trials [2] showed good agreement with analytical solutions and other conventional DSMC codes. Three hypersonic cases considered in the present paper have also shown good agreement with experimental data and the DS3V code, however further work is required to consider permutations of different numerical parameters (e.g. altering the cell size, time step and molecules per particle). A new *Scotch* technique was presented which has the ability to reduce computational time by around 28-35% which will be of benefit to computationally demanding DSMC calculations.

Future work on *dsmcFoam* includes the implementation of the vibrational energy mode and the inclusion of thermo chemistry models. Furthermore, a transient adaptive sub-cell module will be implemented in to *dsmcFoam* to ensure sub-cells are concentrated in regions with higher collision activity, for example, in shock waves and other regions with steep macroscopic gradients. This will result in better resolved DSMC solutions.

## 7. Acknowledgements

The authors would like to thank OpenCFD Limited for their aid in developing the new *Scotch* decomposition technique.

## References

- [1] OpenFOAM: *The open source CFD toolbox*, user guide, version 1.6, www.openfoam.com (2009)
- [2] Scanlon T. J., Roohi E., White C., Darbandi M., and Reese J. M.: An open source, parallel DSMC code for rarefied gas flows in arbitrary geometries. *Computers and Fluids*, **Vol. 39**, Issue 10, pp. 2078-2089 (2010)
- [3] Bird G. A.: *Molecular Gas Dynamics and the Direct Simulation of Gas Flows*, (Clarendon, Oxford, 2009)
- [4] Bird G. A.: Definition of mean free path in real gases. *Physics of Fluids*, **Vol. 26**, Issue 11, pp. 3222-3223 (1983)
- [5] Holden M. S., Wadhams T. P., and Candler G. V., and Harvey J. K.: Measurements in regions of low density laminar shock wave/ boundary layer interaction in hypervelocity flows and comparison with Navier-Stokes predictions. *AIAA Paper 2003-1131* (2003)
- [6] Moss J. N., Bird G. A., and Markelov G. N.: DSMC simulations of hypersonic flows and comparison with experiments. *AIP Conference Proceedings* **Vol. 762**, pp. 547-552 (2004)
- [7] Allègre J., Bisch D., and Lengrand J. C.: Experimental rarefied density flowfields at hypersonic conditions over 70-degree blunted cone. *Journal of Spacecraft and Rockets* **Vol. 34**, No. 6, pp. 714-718 (1997)
- [8] Allègre J., Bisch D., and Lengrand J. C.: Experimental rarefied aerodynamic forces at hypersonic conditions over 70-degree blunted cone. *Journal of Spacecraft and Rockets* **Vol. 34**, No. 6, pp. 719-723 (1997)
- [9] Allègre J., Bisch D., and Lengrand J. C.: Experimental rarefied heat transfer at hypersonic conditions over 70-degree blunted cone. *Journal of Spacecraft and Rockets* **Vol. 34**, No. 6, pp. 724-728 (1997)
- [10] Moss J. N., Glass C. E., and Greene F. A.: DSMC simulations of Apollo capsule aerodynamics for hypersonic rarefied conditions. 9th AIAA/ASM Thermophysics and Heat Transfer Conference. *AIAA Paper 2006-3577*, (2006)
- [11] Bird G. A.: *Visual DSMC Program for Three-Dimensional Flows. The DS3V Program User's Guide, Version 1.2*, March 2005

## 8. Tables

Table 1: Free-stream flow conditions for the two test cases.

Condition	$Ma_\infty$	$T_0$ [K]	$p_0$ [bar]	$\rho_\infty$ [g/m <sup>3</sup> ]	Species	$\lambda_{VHS}$ [m]	Length scale [m]	Knudsen number
Bi-conic case	15.6	2089.6	20.9	0.1757	N <sub>2</sub>	$\approx 2.19 \times 10^{-4}$	0.043	0.005
Planetary probe case	20.2	1100	3.5	0.0173	N <sub>2</sub>	$\approx 1.7 \times 10^{-3}$	0.025	0.067

Table 2: Set-up parameters for the *dsmcFoam* investigations.

Case	Time step (s)	No. mesh cells	No. particles	One particle represents	Processors used	Time taken to reach steady state
Bi-conic case	$\approx 5.89 \times 10^{-8}$	$\approx 3 \times 10^6$	$\approx 91.8 \times 10^6$	$\approx 3.3 \times 10^{11}$ molecules	64	$\approx 28$ hours
Planetary probe case	$\approx 1.3 \times 10^{-7}$	$\approx 7.7 \times 10^6$	$\approx 79.9 \times 10^6$	$\approx 1.3 \times 10^{10}$ molecules	64	$\approx 2.8$ hours
Apollo capsule	$1.7 - 3.6 \times 10^{-6}$	$\approx 4.3 \times 10^6$	$\approx 4.7 \times 10^7$	$\approx 4.1 \times 10^{14}$ molecules	32	$\approx 5$ hours

Table 3: Surface temperatures of the different cases.

Investigation	$T_w$ [K]
Bi-conic case	297.2
Planetary probe case [7]: density flowfield	290
Planetary probe case [8]: drag coefficient	350
Planetary probe case [9]: heat transfer	300

Table 4: Free-stream velocities incurred by the Apollo capsule at an altitude of 105 km.

$V_\infty$ , m/s	$T_w$ , K	$C_{m,0,dsmcFoam}$	$C_{m,0,Moss\ et\ al.\ [10]}$
7680	871	0.1134	0.113
8290	922	0.1136	0.113
9600	1029	0.1137	0.113
10759	1121	0.1139	0.113
15000	1439	0.1140	0.113

Table 5: Atmospheric composition and free-stream condition incurred by the Apollo capsule at an altitude of 105 km.

$\rho_\infty$	$n_\infty$	Molecular weight	$T_\infty$ , K	$X_{O_2}$	$X_{N_2}$	$X_O$
$2.364 \times 10^{-7}$	$5.0947 \times 10^{18}$	27.943	208	0.15808	0.78319	0.05873

## 9. Figures

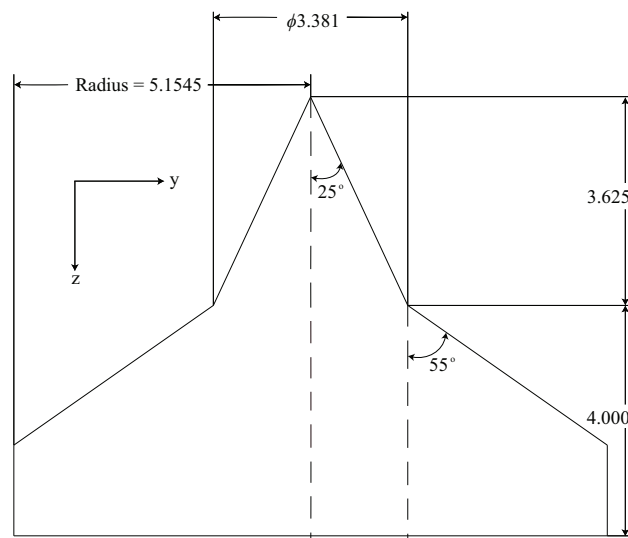


Figure 1: 25°/55° bi-conic cylindrical object configuration. Dimensions are in inches.

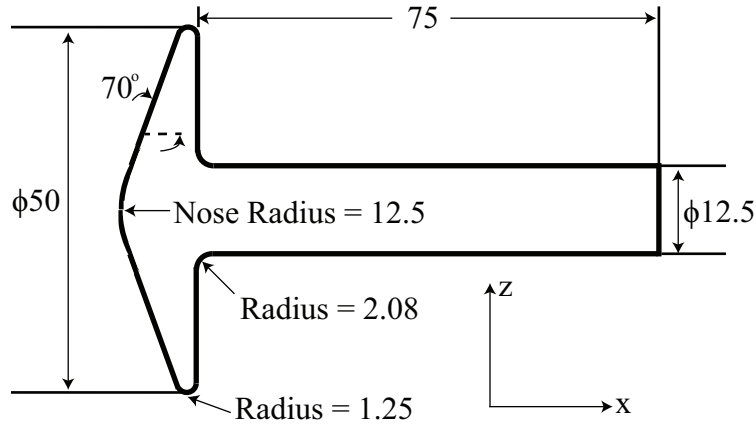


Figure 2: Planetary probe configuration. Dimensions are in millimetres.

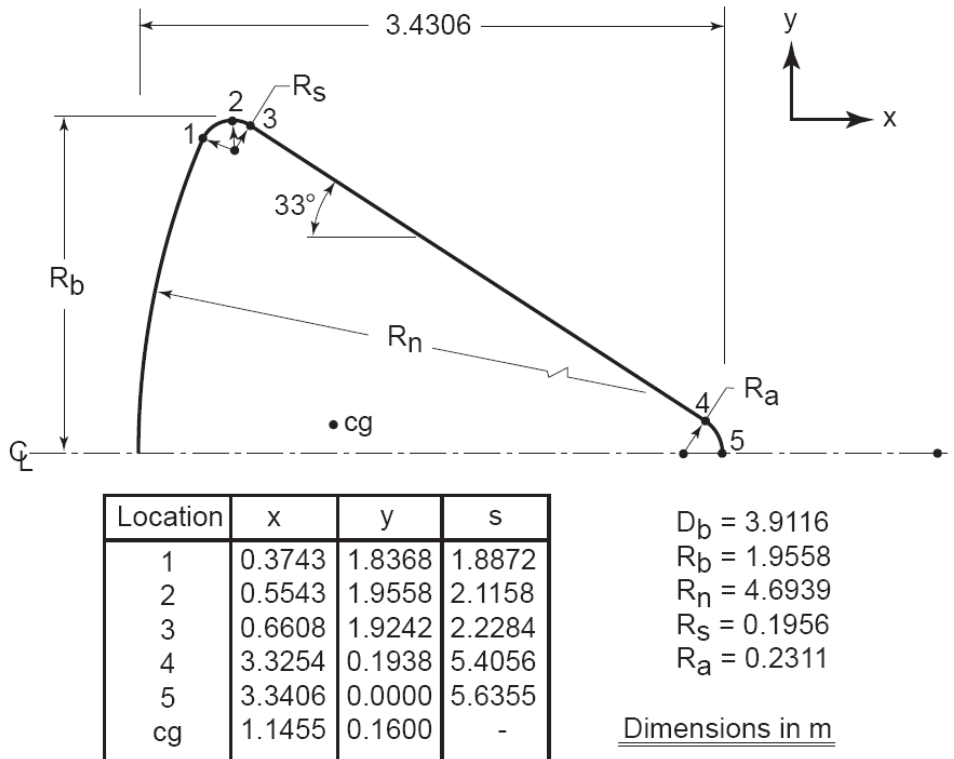


Figure 3: Apollo Command Module configuration [10]. cg stands for the center of gravity. Note, we believe location 5 should have an x value of 3.4306 instead of 3.3406.

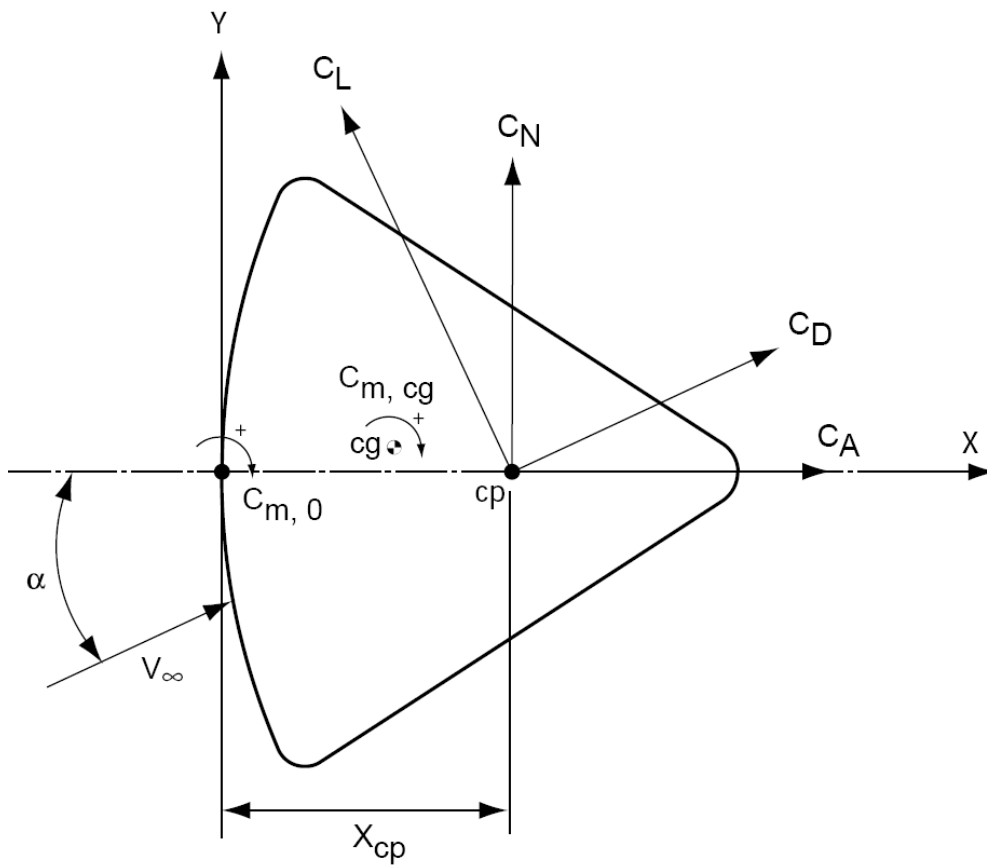


Figure 4: Pitch plane aerodynamic forces on the Apollo Command Module [10].

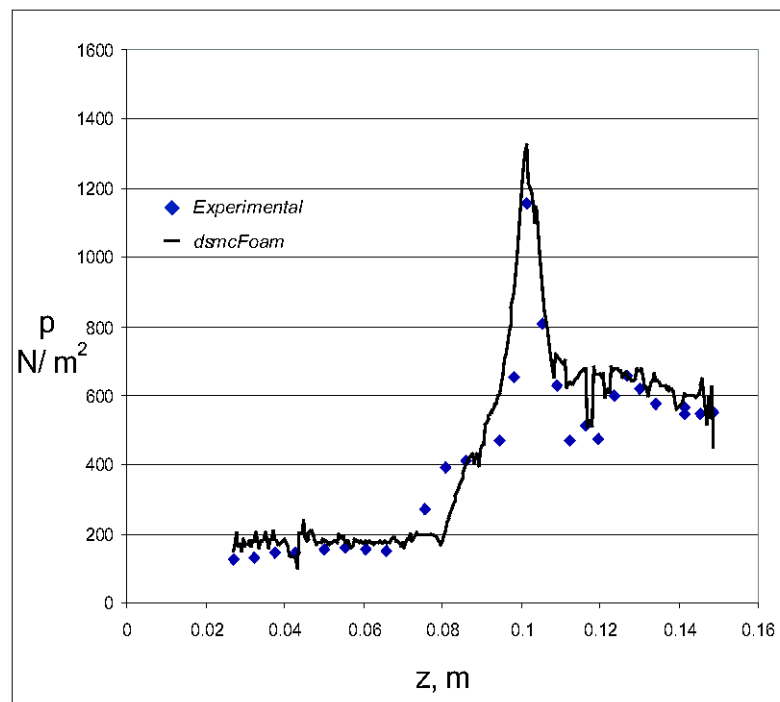


Figure 5: Bi-conic case: comparison of experimental data and *dsmcFoam* calculations of surface pressure.

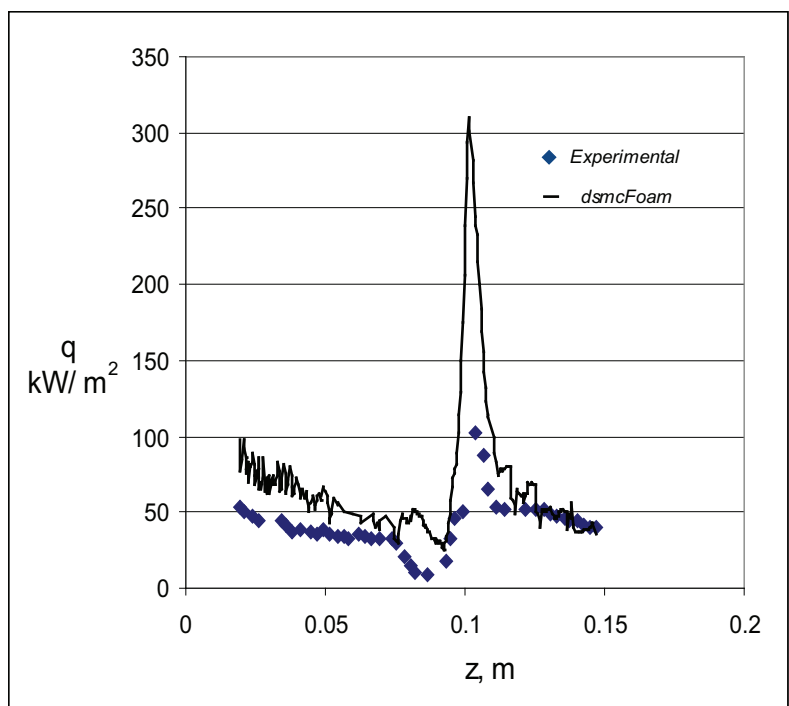


Figure 6: Bi-conic case: comparison of experimental data and *dsmcFoam* calculations of surface heat transfer.

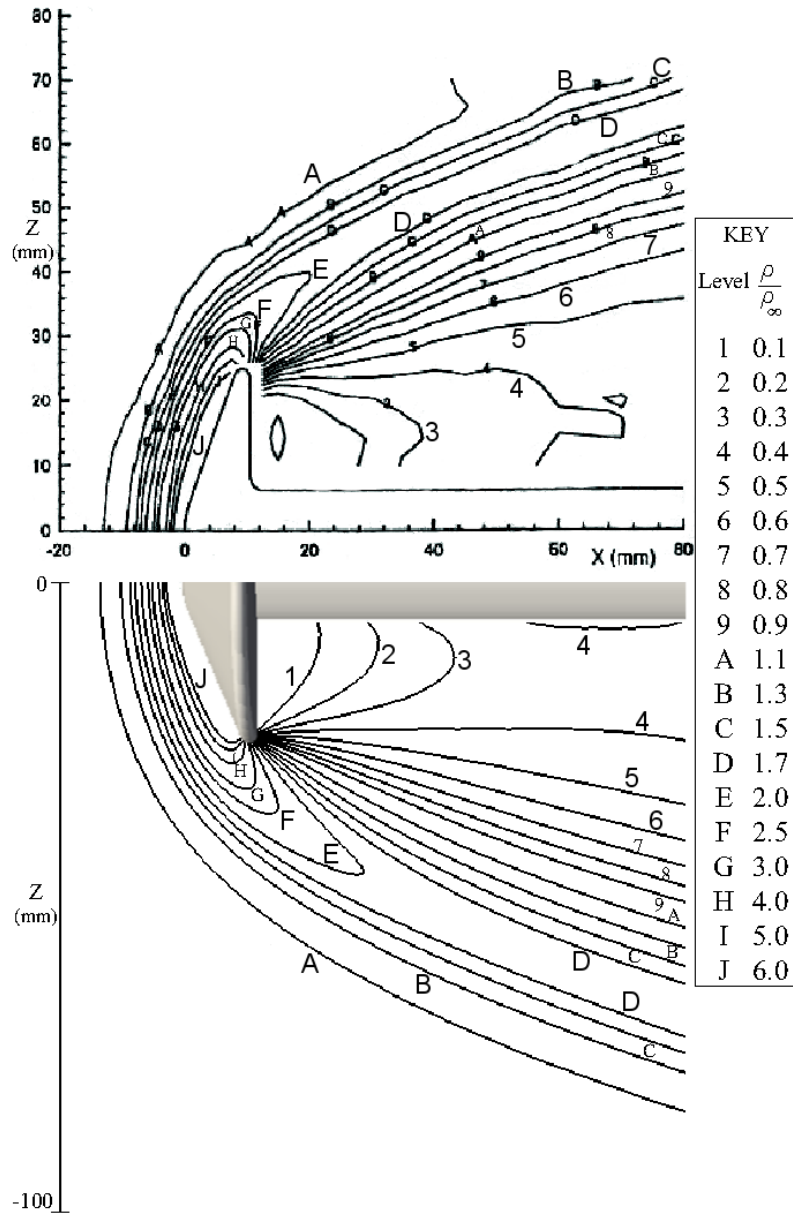


Figure 7: Planetary probe at zero angle of attack: comparison of experimental data (top half) and *dsmcFoam* calculations (bottom half) of dimensionless density profiles

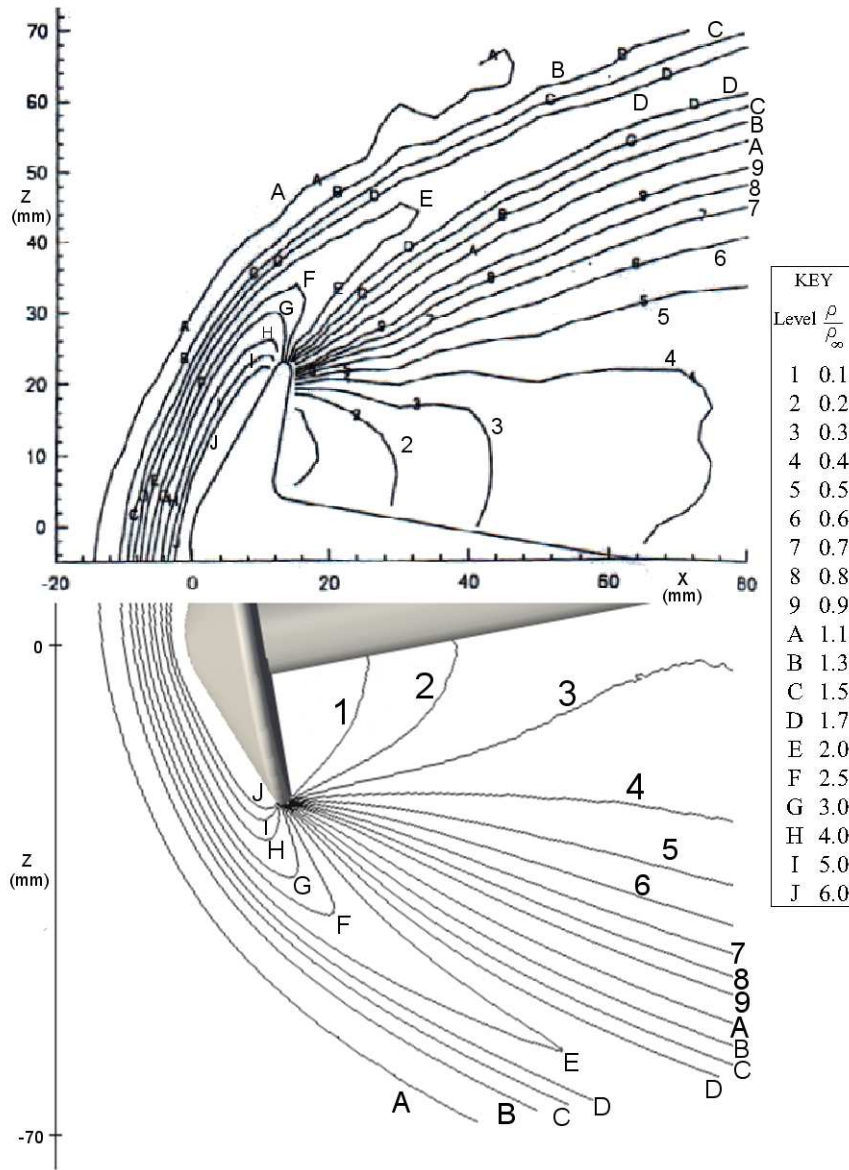


Figure 8: Planetary probe at 10 degrees angle of attack : comparison of experimental data (top half) and *dsmcFoam* calculations (bottom half) of dimensionless density profiles

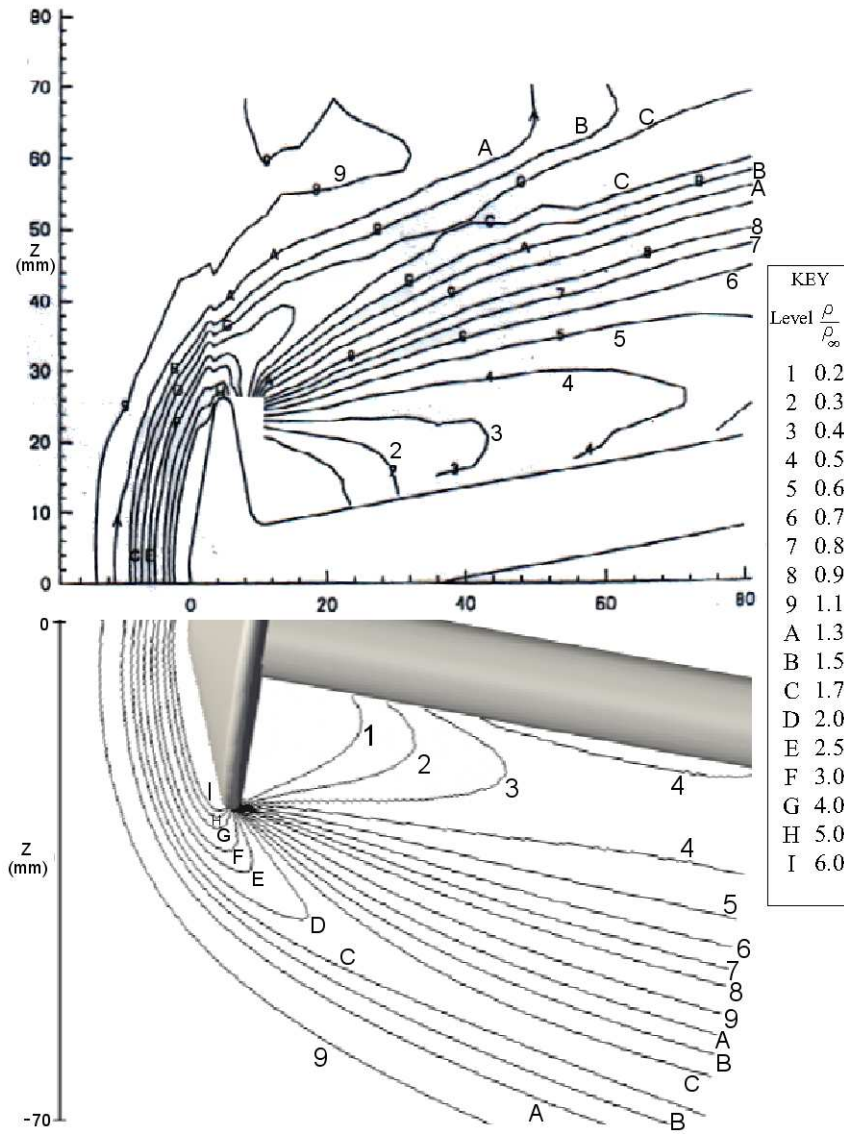


Figure 9: Planetary probe at -10 degrees angle of attack: comparison of experimental data (top half) and *dsmcFoam* calculations (bottom half) of dimensionless density profiles

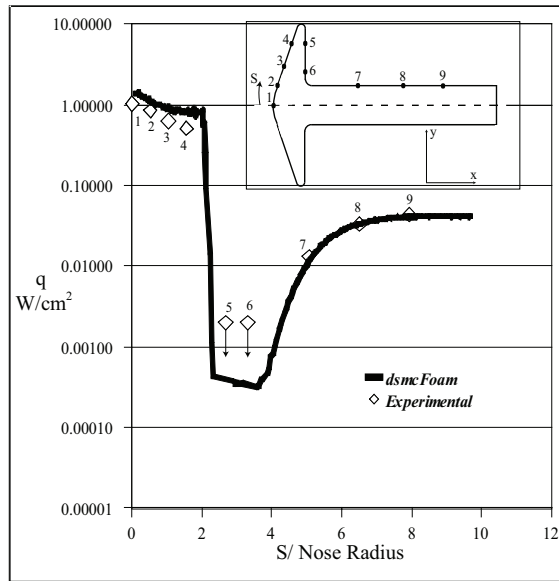


Figure 10: Planetary probe at zero angle of attack: comparison of experimental data and *dsmcFoam* calculations of surface heat transfer.

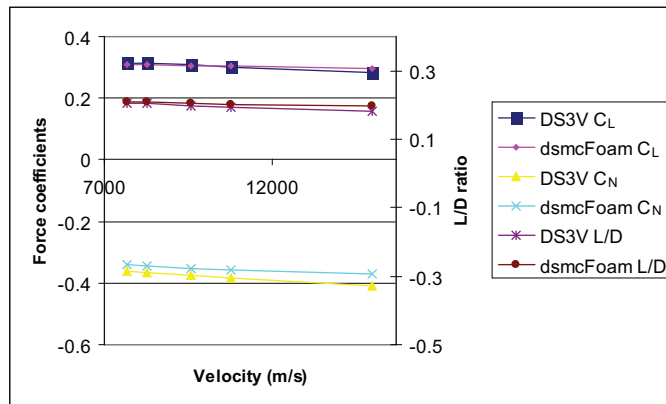


Figure 11: Apollo capsule: comparison of *dsmcFoam* and DS3V calculations of aerodynamic coefficients and lift to drag ratio.

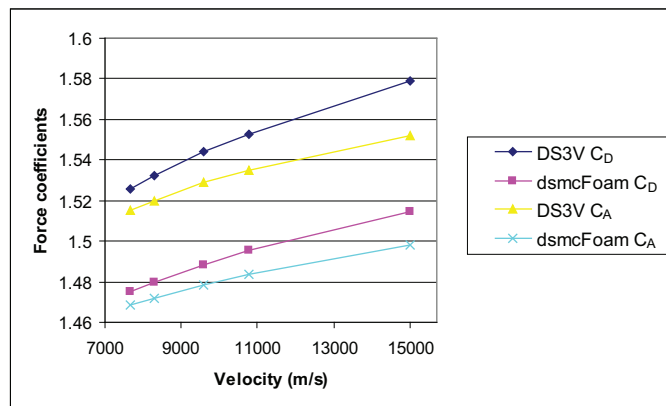


Figure 12: Apollo capsule: comparison of *dsmcFoam* and DS3V calculations of aerodynamic coefficients.

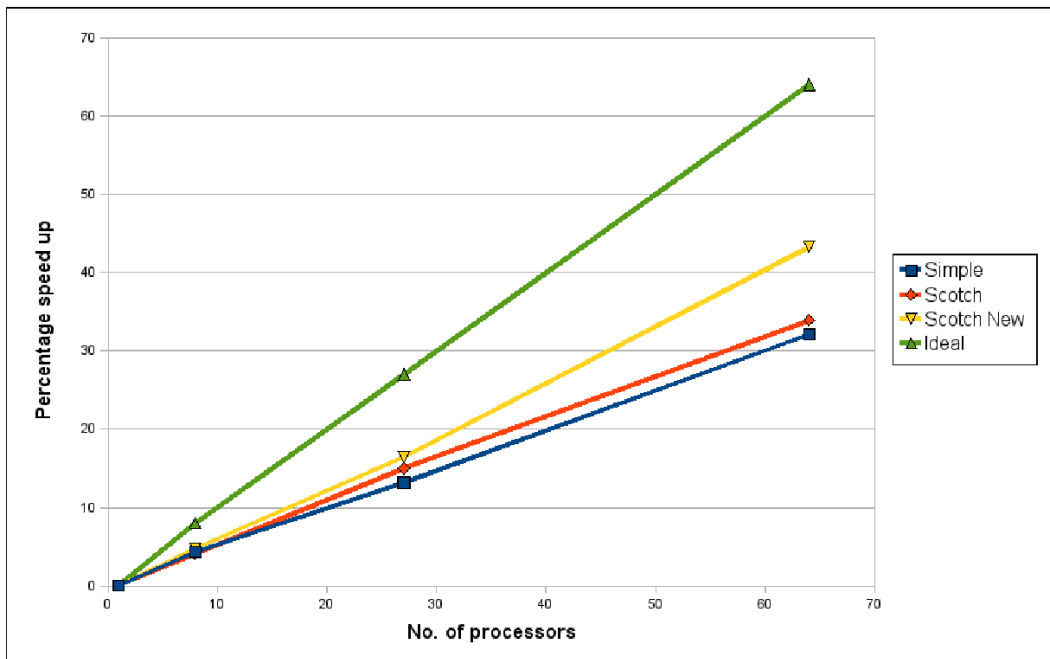


Figure 13: Percentage speed up comparisons of three decomposition techniques tested on the zero angle of attack planetary probe case.